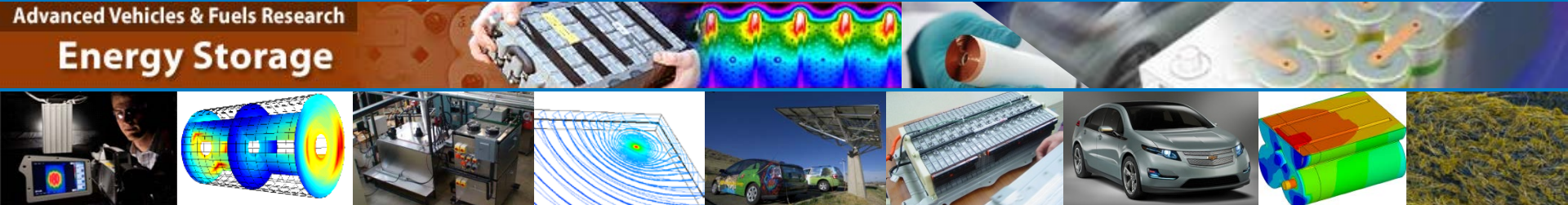


Modeling Lithium Ion Battery Safety: Venting of Pouch Cells

Advanced Vehicles & Fuels Research
Energy Storage



Shriram Santhanagopalan, Chuanbo Yang

Task Leader: Ahmad Pesaran

*National Renewable Energy Laboratory
July 2013*

*NREL Deliverable Report in fulfillment of July 2013 Milestone
Titled "Complete Case-Studies on Pouch Cell Venting"
Energy Storage Task 3.2: "Component Level Models for Lithium Ion Battery Safety"*

Foreword

This report documents the successful completion of the NREL July milestone entitled “Modeling Lithium-Ion Battery Safety - Complete Case-Studies on Pouch Cell Venting,” as part of the 2013 Vehicle Technologies Annual Operating Plan with the U.S. Department of Energy (DOE).

This work aims to bridge the gap between materials modeling, usually carried out at the sub-continuum scale, and the Multi-Scale-Multi-Domain (MSMD) models. In FY12, we developed component models for the electrodes, interfaces, electrolytes, etc., that incorporate the material properties calculated from micro-scale simulations to establish this connection. In FY13, these component models were integrated into cell-level simulations. As the first set of case studies to demonstrate the utility of these models, venting in-pouch format lithium-ion cells under different abuse scenarios was simulated. The build-up and distribution of pressure within the cell is calculated from the component-level models. Gas evolution at the electrode/electrolyte interface as a function of parameters like surface roughness and electrolyte viscosity are included. The cell-level response is then calculated using these estimates.

Some preliminary experimental data collected in collaboration with Sandia National Laboratories and the Johnson Space Center at NASA are compared to the model predictions.

The Energy Storage Program of the DOE Office of Vehicle Technologies funded this work. We wish to thank our sponsors David Howell and Brian Cunningham for their support.

Ahmad Pesaran
Energy Storage Task Leader, NREL
(303) 275-4441; ahmad.pesaran@nrel.gov

Executive Summary

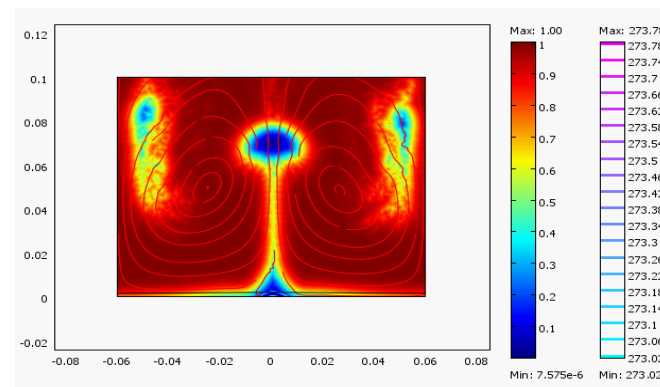
- **Lithium-ion batteries swell under several abuse conditions, such as overcharge, contamination of the cell with traces of moisture, or overheating.**
- **Given the poor understanding of the swelling mechanism and the limited control over the quality of the seals, pressure build-up poses a serious issue for batteries encasing multiple cells within the same container.**
- **This report integrates mathematical models for individual factors that contribute to the swelling of lithium-ion cells, and relates the pressure value within the cell to the mechanical strength of the casing.**
- **Comparison to preliminary experimental data is included. Future work will focus on developing reproducible methodology to reduce uncertainty in the test results.**
- **Applications of these models include:**
 - Realistic prediction of battery safety under extreme conditions
 - Identification of the gaps in the cell fabrication process and providing a rational means of building quality control measures for the sealing of the cell casing
 - Identification of failure mode during destructive physical analysis of cells that fail safety testing in the laboratory.
- **The proposed solution is not specific to a given chemistry or cell design, and thus will be applicable to state-of-the-art or future battery chemistries and designs.**

Objective & Rationale

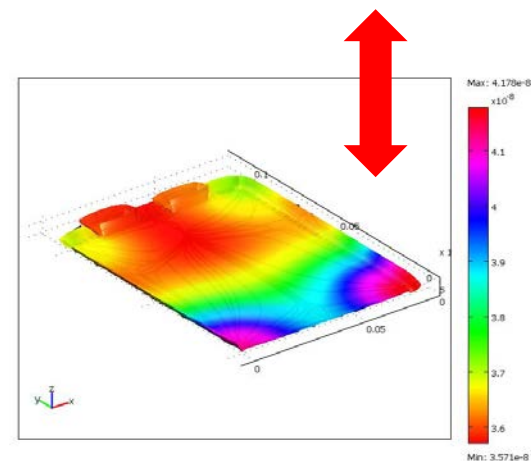
- **The objective is to build a single simulation tool that is useful in identifying material limitations and assessing design modifications in cell fabrication side by side to improve the safety margin of lithium-ion batteries.**
- **The integrated model will provide a realistic assessment of the impact the choice of materials and operating conditions will have on the improvements to battery safety.**
- **Some modifications to the traditional approach of modeling cell components were introduced in the previous years' work to accomplish such integration:**
 - Pressure generation from various cell components due to chemical reactions and electrochemical degradation taking place within cells subjected to abuse were developed
 - Simulation of point defects (e.g., short circuit) were carried out in realistic cell geometries, enabling one to study the interaction of design aspects at the cell level with artifacts of the chemistry
- **In the current year, we have used these models to simulate venting of the cells under extreme pressure conditions. Case studies to isolate cell failure and improve cell design were developed.**
- **This tool will help cell manufacturers compare various options available for improving the safety of their cell design in a methodical fashion.**

Background

- **In FY12:**
 - ✓ NREL built mathematical tools to relate the material response on the electrode surface to cell-level phenomena.
 - ✓ The detailed microstructure model replaced the single spherical particle approximation commonly used in literature to simulate behavior at the particle level.
 - ✓ The cell-level application of the model was demonstrated using pressure build-up due to overcharge as a case study.
- **In FY13:**
 - ✓ Correlated the mechanical strength of the cell packaging with the pressure build-up models for various form factors
 - ✓ Developed simulation tools to capture physical deformation of the cell (e.g., during events like cell venting)
 - ✓ Identified model parameters that can be used as quality control metrics during the cell fabrication process
 - ✓ Made some preliminary comparison to cell-level experimental data.



Electrolyte decomposition and gas evolution on an electrode surface



Unequal distribution of reaction rates and pressure within the cell during overcharge

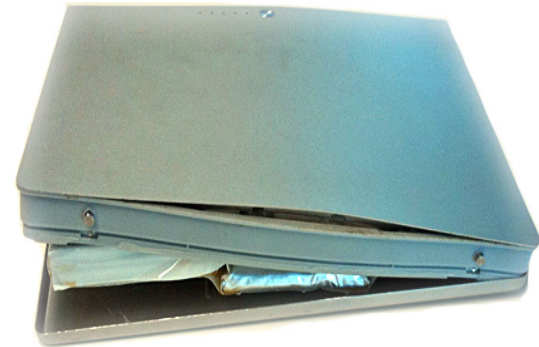
FY12 Recap: Relating Material Response to Cell Level Phenomena under Li-Ion Battery Abuse Scenario

Pressure Buildup in Lithium-Ion Cells

Pressure buildup/cell venting is the most common response observed in lithium-ion batteries subjected to abuse:

Overheating:

- Heating of the cell results in vaporization of the organic solvents used in the electrolytes.
- Additional degradation modes are activated due to the chemical reaction between the electrolyte and the cell components resulting in expedited gas generation.
- Mechanical compliance of electrodes, casing, and separator is lowered.



Mechanical Damage:

- The most commonly observed consequence of mechanical damage (e.g., due to a crush or short circuit) is rapid buildup of pressure within the cell due to the runaway reactions, resulting in venting of the cell even in cases where the container is not compromised due to the initial mechanical event.
- Faulty seals in hard-case cells often result in contamination of the cell with traces of moisture, which subsequently reacts with the electrolyte, resulting in additional pressure buildup.

Overcharge:

- Aggravated kinetics at extreme temperatures for the charge transfer reaction results in additional wear and lowers the voltage stability for the electrolyte, resulting in breakdown of the electrolyte into gaseous species.
- At lower stoichiometries that result during overcharge, some transition metal oxide cathodes readily release oxygen from the host lattices.



Simulating Pressure Buildup

- Previously, we simulated the buildup of pressure due to gas bubbles generated from chemical reactions during overcharge using a jump momentum balance for the interface:

$$f^i = -\mathbf{n} \cdot \left(P^i \mathbf{I} + \eta \left[\nabla \mathbf{u}^i + (\nabla \mathbf{u}^i)^T \right] \right)$$

where pressure in the source term (P^i) was calculated using Faraday's law and gas laws.

- This model was made sufficiently generic to accommodate:
 - phase changes due to evaporation and
 - source terms for the pressure either from within an individual phase or from the boundaries
- The pressure term in the momentum balance equation becomes:

$$P^i = P_1^i + P_2^i + P_3^i$$

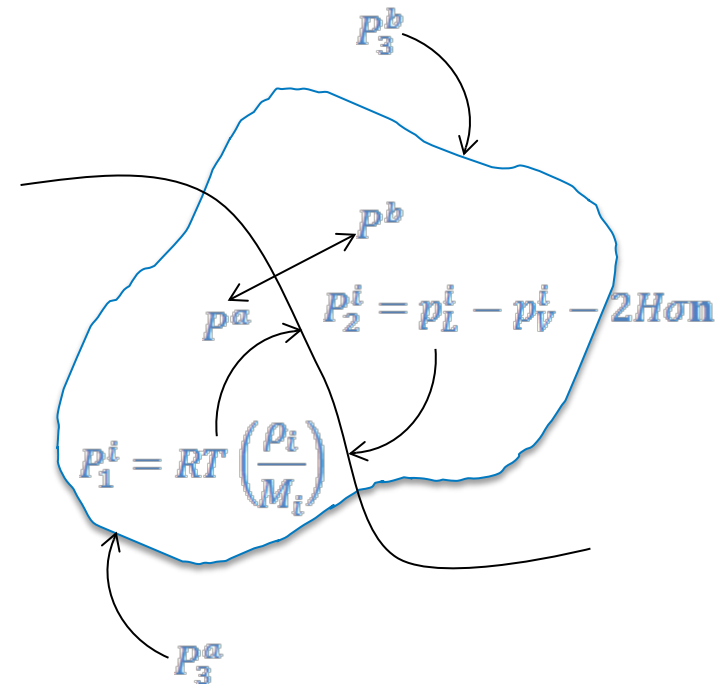
where

$P_1^i = RT \left(\frac{\rho_i}{M_i} \right)$ is the pressure from gas generating reactions.

$P_2^i = p_L^i - p_V^i - 2H\sigma n$ is the pressure due to evaporation of organic solvents; the partial pressures in the liquid and vapor phases (p_L^i and p_V^i) can be computed readily using vapor-liquid equilibrium data available in standardized tables.


P_3^i is the pressure exerted by the casing on the jellyroll and the fluid phase within the cell – this is described in more detail in the next few slides.

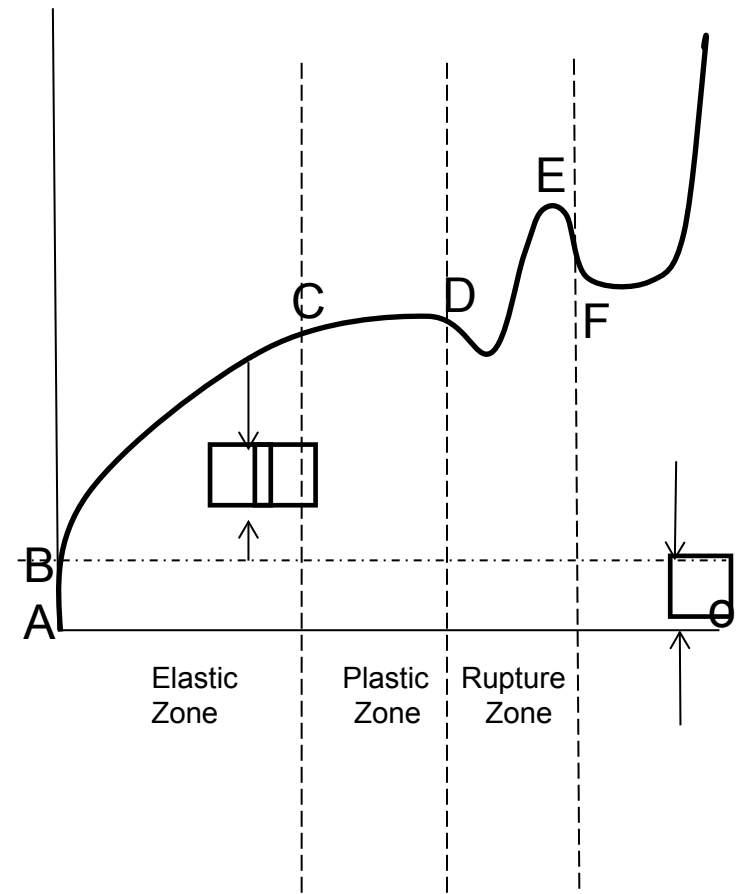
- In our previous overcharge simulations, we set $P^i = P_1^i$ (i.e., we assumed $P_2^i = P_3^i = 0$).



Pressure build-up within a pouch format lithium-ion cell: the contributions from the individual components are compared against the total pressure within the cell in the next few slides.

Mechanical Strength of the Cell Casing

- The deformation of the cell container imposes two additional source terms to the pressure developed within the cell:
 - The change in the volume of the cell results in alleviation of the cell pressure.
 - The rigidity of the mechanical casing results in additional constraints on the fluid volume within.
- The former can be calculated once the force imposed by the casing is known. We represent this interfacial value for the force as p_3^I in the previous slide.
- The stress-strain curve for the individual cell components and that for the casing material can be measured independent of the cell configuration. A sample curve showing the ultimate and yield strengths for an elastic material is shown alongside.
- As long as the stress on the casing continues to remain below point E on the curve, the net result is a deformation by  which results in subsequent wrinkles on the cell surface when the internal pressure within the cell is lowered again (e.g., cooling of the cell after the exposure to high temperature).
- However, once the pressure value crosses E, the strain value increases instantaneously, resulting in unequal stresses across the seal/weld.



Elastic-plastic deformation of the cell casing:

- D Yield strength
- E Ultimate strength
- F Fracture

Effect of Casing Strength on Cell Pressure

- The mechanical response shown in the stress-strain curves is captured using the following relationship:

$$\Delta\sigma = \sigma - \sigma_0 = D(\epsilon - \epsilon_{th} - \epsilon_p - \epsilon_0)$$

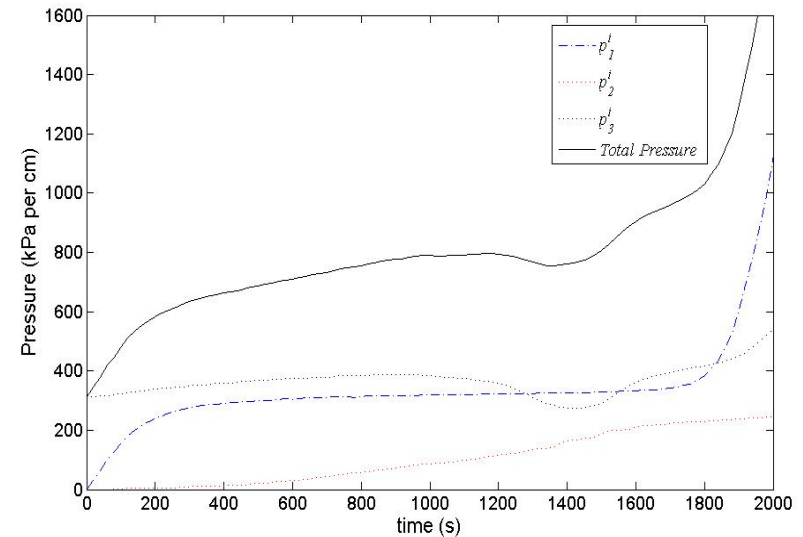
Here σ and ϵ are the stress and per-unit volume; D , σ_0 , and ϵ_0 are functions of material properties like Young's modulus and Poisson's ratio; ϵ_{th} and ϵ_p are the correction factors for the thermal influence and plasticity of the material.

- Expansion of the cell by $\Delta\epsilon = \epsilon - \epsilon_{th} - \epsilon_p - \epsilon_0$ results in the pressure within the cell dropping by $\Delta\sigma$. Thus, we have:

$$P_3^i = -\Delta\sigma \cdot n$$

as the expression relating the contribution of the cell casing strength towards the pressure within the cell. From the stress-strain curves shown on slide 8, this corresponds to a gradual decrease in the pressure, followed by an increase along the compliance regime, a second drop, and then zeroing out of the pressure due to the cell venting.

This trend is influenced by the other factors (i.e., p_1^i and p_2^i , which, in turn, correspond to the effect of chemical composition and the ambient temperature on the pressure generation within the cell).



Development of pressure within a pouch cell:

P_1^i is the pressure generated from decomposition of the electrolyte and other reactions generating gaseous species

P_2^i is the pressure component from the evaporation of volatile species within the cell

P_3^i is the contribution from the cell mechanical toughness of the casing imposing stresses on the jellyroll

Numerical Implementation

- As in our previous years' efforts, a level-set scheme is used to numerically implement the growth of the gas-liquid interface:

$$\frac{\partial \varphi}{\partial t} + \nabla \varphi \cdot \mathbf{u} = \gamma \nabla \cdot (\epsilon \nabla \varphi - \varphi(1 - \varphi) \mathbf{n})$$

where the level-set variable φ takes the form of a smooth function varying between zero for one phase and one for the other phase.

- An arbitrary Lagrangian-Eulerian scheme minimizes the need for re-meshing the deformed geometry at each time step, thereby providing adequate computational efficacy.
- The pressure value at each spatial location is calculated as the summation of the contributions from the individual species:

$$P(\xi, t) = \sum_i P^i(\xi, t)$$

- Scaling up from one level to another (e.g., the component to the cell level), an “effective” or average value of pressure is computed for each element and fed as a source term to the momentum balance at the higher level:

$$\bar{P}(t) = \frac{1}{V(t)} \int_{V(t)} \left\{ \sum_i P^i(\xi, t) \right\} \left(\frac{A^i}{\sum_i A^i} \right) dV(t)$$

Material Properties

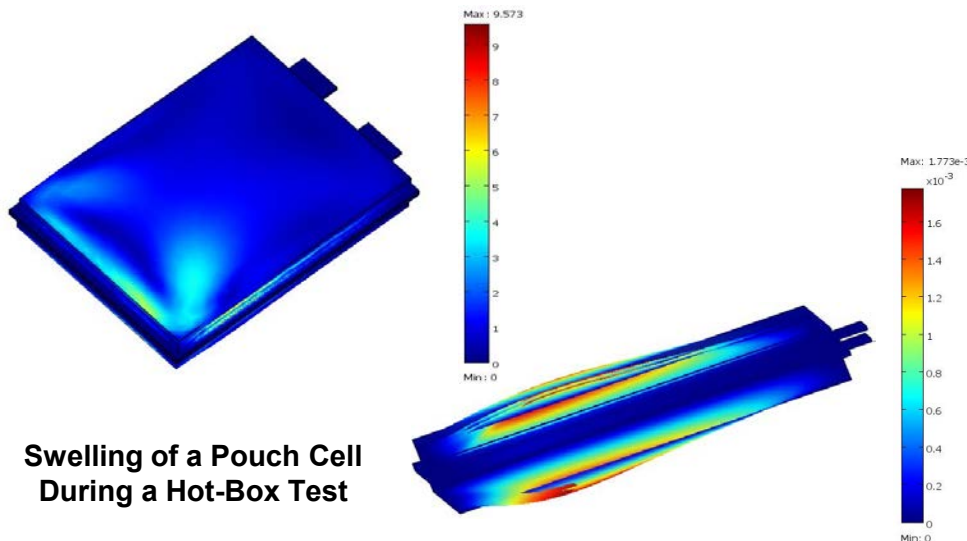
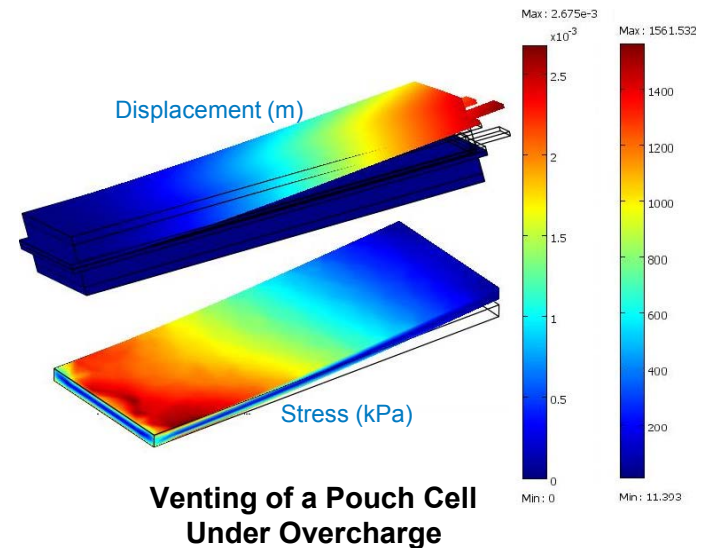
Mechanical Properties	Units	Al Current Collector	Cu Current Collector	Positive Active Material	Negative Active Material	Separator
Modulus of Elasticity	MPa	70,000	110,000	10,000	10,000	3,450
Tangent Modulus	MPa	700	1,100	100	100	35
Poisson Ratio	--	0.36	0.35	0.3	0.3	0.35
Weight Density	lb/in ³	0.097504	0.287	0.1518	0.0803	0.0426
Mass Density	Tonne/mm ³	2.699e-9	7.944e-9	4.202e-9	2.223e-9	1.179e-9
Yield Stress	MPa	180	210	100	100	18
Yield Strain	%	1.7	2.2	5.6	5.6	6
Ultimate Stress	MPa	195	230	110	110	180
Ultimate Strain	%	2.7	3.5	8	8	250
Reference	--	1,2	1,2	3,5	3,5	1,2,4

References:

1. Richard Hill, PhD Dissertation, Massachusetts Institute of Technology, 2011.
2. www.matweb.com, Last accessed May 2013.
3. J. Christensen and J. Newman, J. Electrochem. Soc., Vol. 153(6), p. A1019-1030, 2006.
4. C. Lotti et al., European Polymer Journal, Vol. 44, p. 1346-1357, 2008.
5. V. Battaglia, Presented at the DOE Annual Merit Review, Washington D.C., 2010.

Case (i): Venting in Pouch Cells

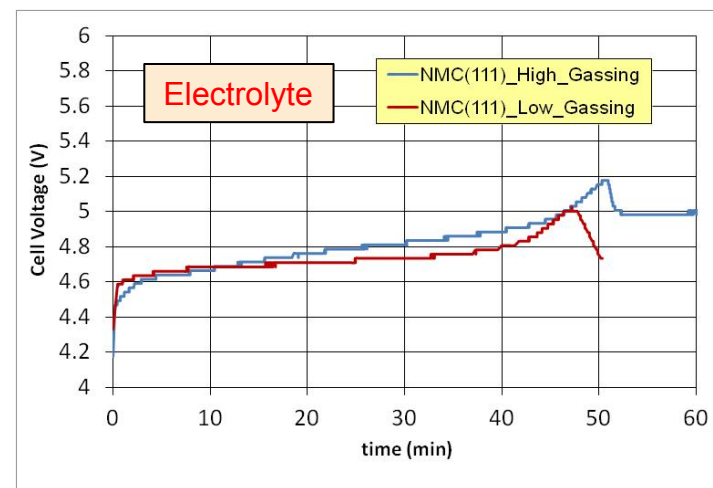
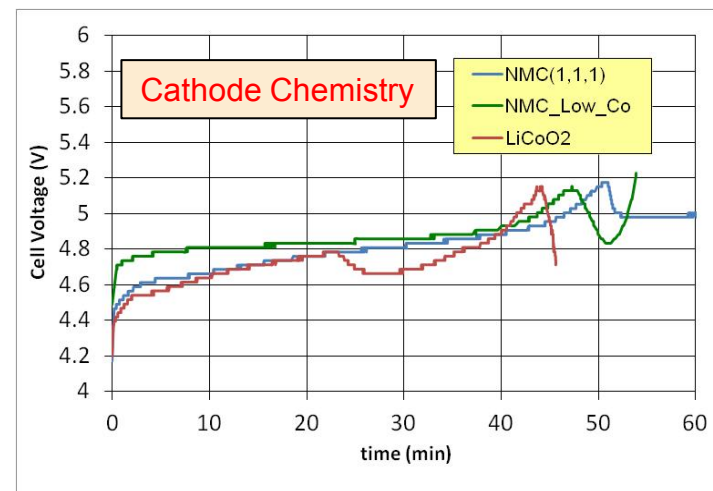
- To demonstrate the versatility of the model, the parameters shown in the previous slide were used to simulate the mechanical response of a pouch cell subject to overheating, ball crush, and overcharge.
- Simulation results for the swelling of the cells during a hot-box test is shown below, including the uneven displacement across the cell walls corresponding to the pressure accumulation.
- The order of magnitude for the pressure within the cells is much smaller compared to those from overcharge.



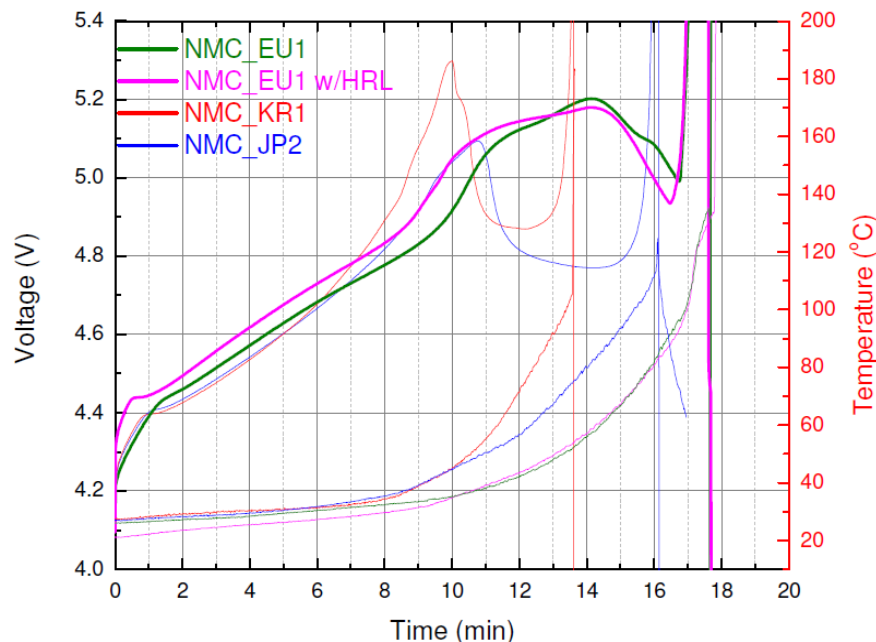
- Venting of the cell originates across the seals close to the tabs, which is mechanically the weakest point on the cell container.
- Venting of the pouch releases excess pressure across the jellyroll, as expected.
- The effect of the P_3^t term (i.e., the impact of cell wall on the jellyroll) is visible on the stress distribution plot across the jellyroll.

Chemistry vs. Overcharge Response

- Voltage vs. time curves during overcharge are different for cells of different designs, even with the same chemistry.
- This feature is incorporated into the models by including different rate expressions for the different ratios of Ni, Co, and Mn.
- This approach, together with the impedance change within the cell due to the pressure accumulation, helps identify the reason for failure during overcharge of the cells.



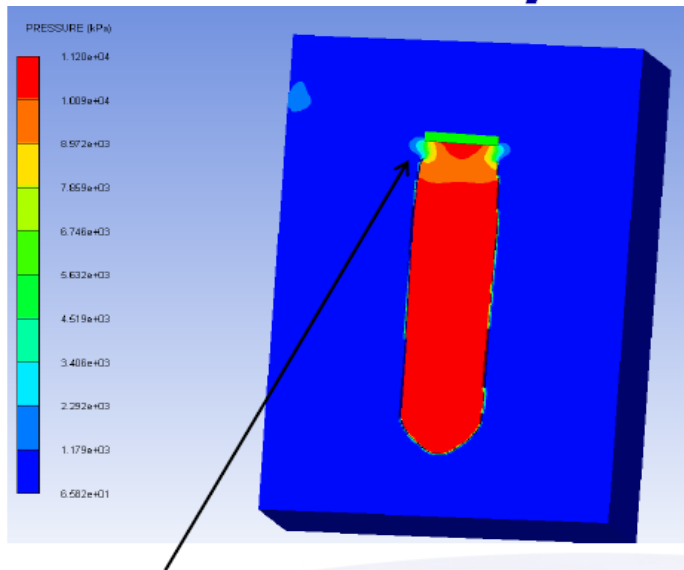
Simulation Results



Experimental Data

Case (ii): Cylindrical Cells

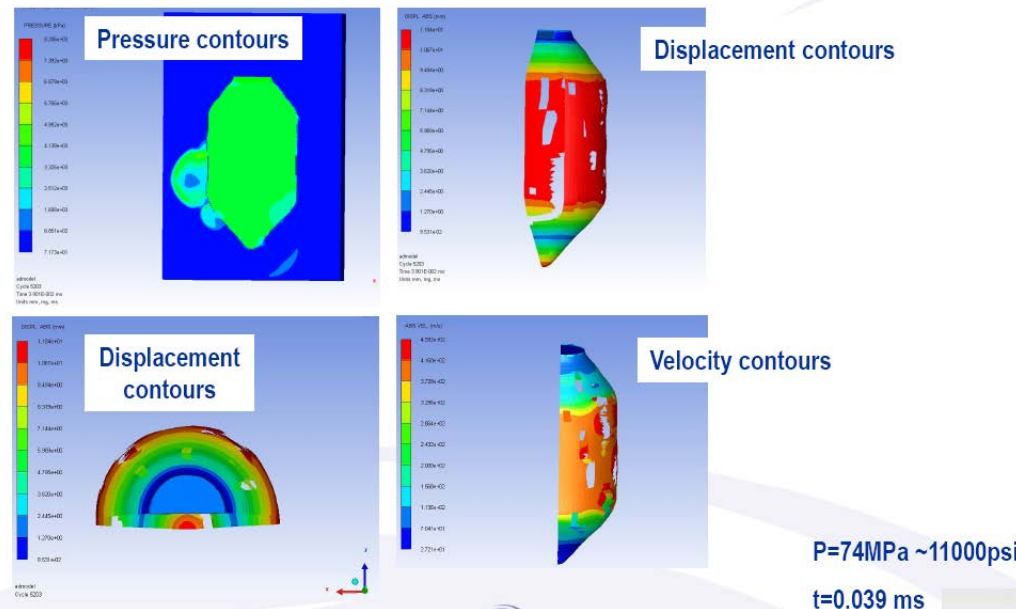
Simulations: Crimp Failure



High pressure gas forces open crimp and ejects top (header)

- We demonstrated the abuse response of cells with cylindrical geometry in an earlier report.
- The results from these models are in agreement with our current results (magnitude of pressure and the location of the point of failure).

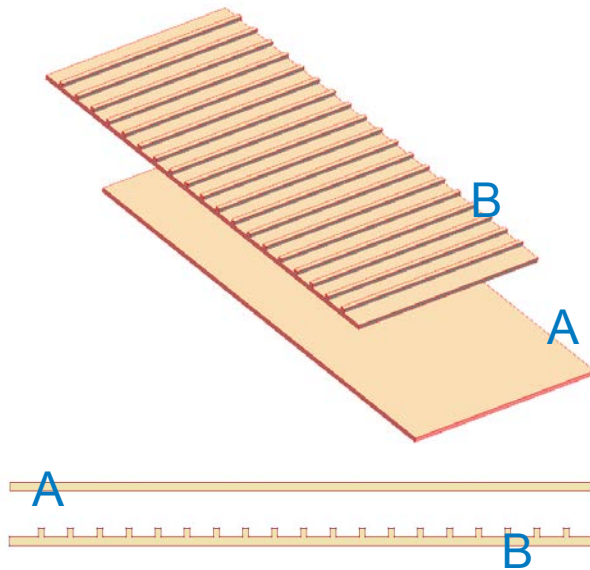
Simulations: Can Failure



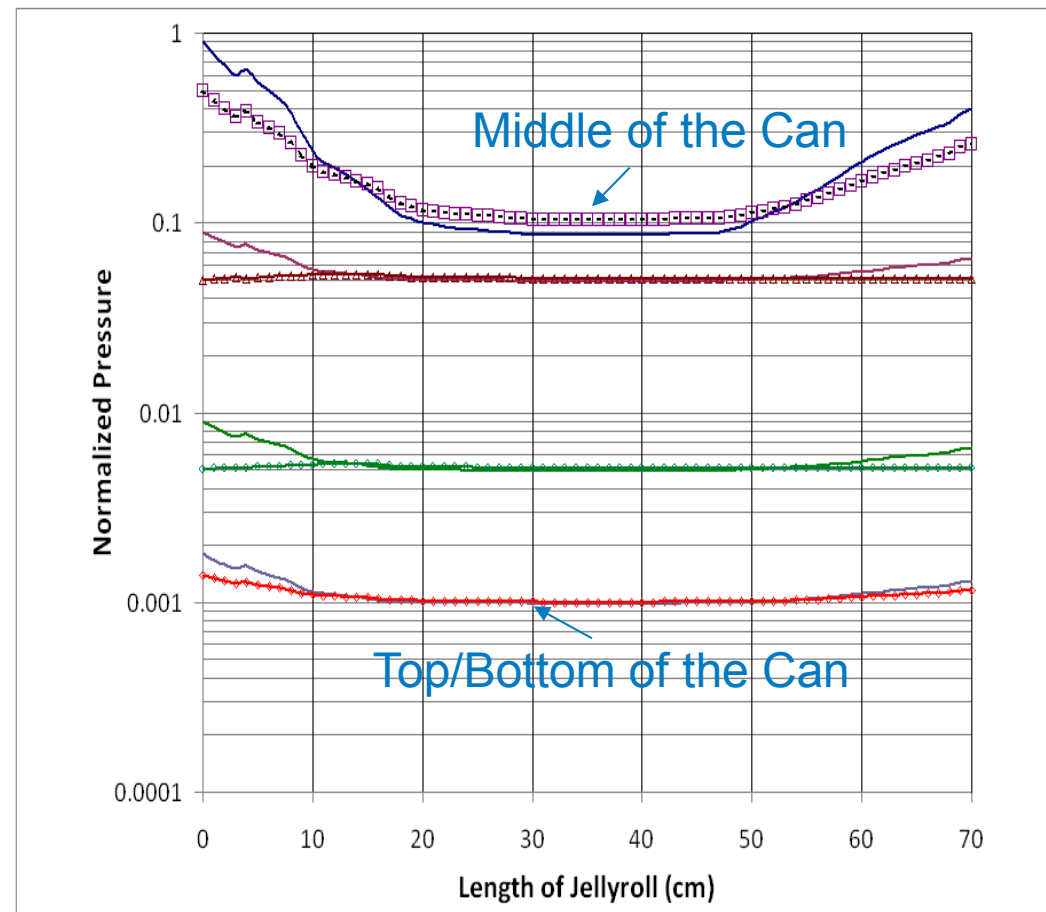
- Invariably, the cells fail due to the mechanical compromise along the crimp region. Can failure was not observed for any of the cases we simulated.

Cell failure models built in 2010 under an STTR from the Navy with Oceanit, LLC. Then, the model used assumed values for pressure within the cells.

Mitigation of Pressure in Wound Cells



- Pressure buildup and distribution across the length of the jellyroll can be mitigated by introducing micron-sized grooves at the interface of the electrode and the separator.
- The models predict a lowering of the pressure along the mid-section of the can.
- There is room for optimizing the size/positioning of the grooves.



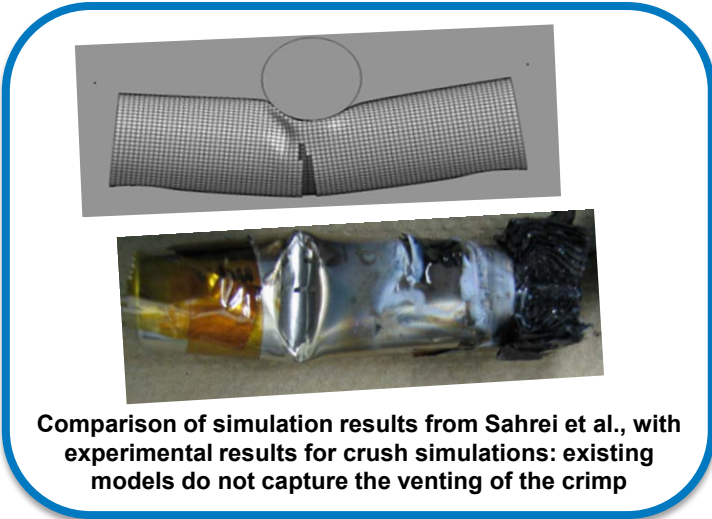
Pressure profiles across the height and length of the electrodes: the lines without symbols represent Case A (no grooves) and those with the symbols represent Case B (with grooves).

Case (iii): Crush Simulations

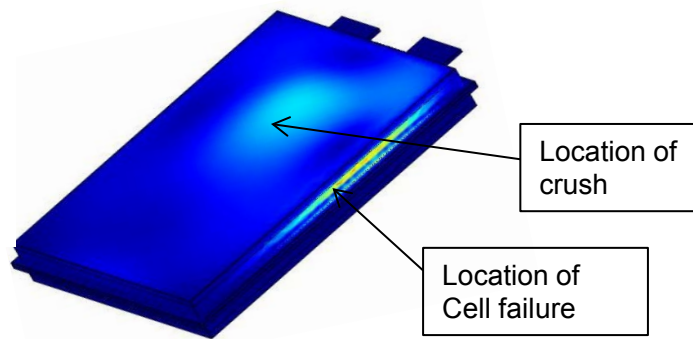
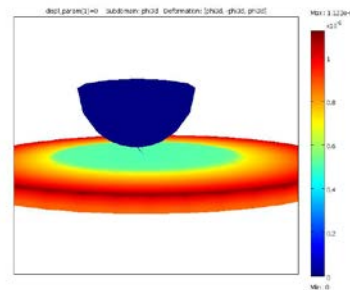
- Sahrei et al. have identified mechanical failure at the point of crush as the failure mode for prismatic and cylindrical cells.
- These results, based on a purely mechanical standpoint, are valid for cells at low states of charge or under the hypothetical scenario when there is no current flow across the induced short.
- To capture the propagation of the short from one cell to others within the pack, subsequent thermal response of the cell should include the reaction kinetics.
- For example, as pointed out on Slide 14, for cylindrical cells, the mode of failure for the cell was invariably venting of the cell across the crimp, irrespective of the location of the short – this increases the likelihood of propagation along the axial direction, rather than radial failure as observed by Sahrei and co-workers.



Sahrei, Campbell and Wierzbicki, J. Power Sources, Vol. 220, p. 360-372, 2012.



Comparison of simulation results from Sahrei et al., with experimental results for crush simulations: existing models do not capture the venting of the crimp



Stress distribution from NREL simulations show that for propagation purposes, the location of cell failure does not always coincide with the location of crush!

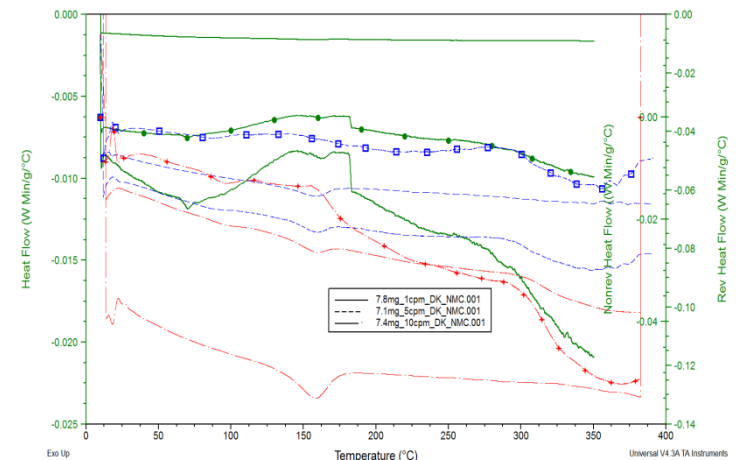
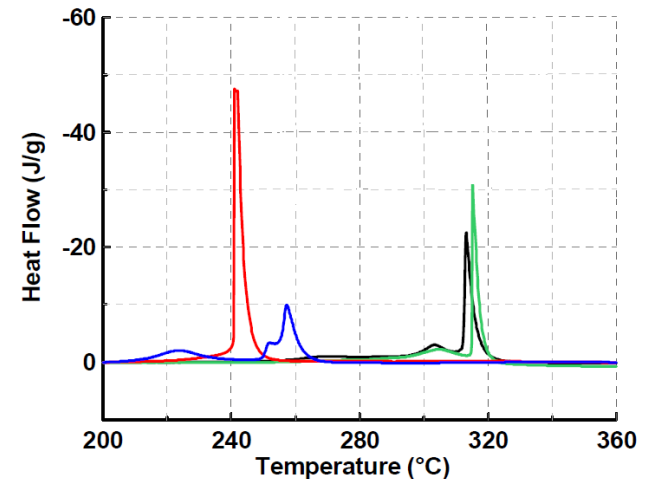
- These results have implications for designing the test methods for evaluating crush-induced failure.

Work in Progress...

Measurement of Parameters for Abuse Reactions:

- Heat generated as a function of time and cell temperature will serve as input to our chemical reaction models used to predict the abuse response of the battery
- This data was obtained for the NCA, NMC and LiCoO₂ (baseline) chemistries using differential scanning calorimetry (DSC) experiments.
- Summary of the heat gen. characteristics is provided below; the transient data will be fed to a kinetic model as the source term.
- Modulated DSC measurements to isolate irreversible (kinetic) heat components from the reversible (enthalpy) components are underway.

Cathode	Peak Temp. (deg. C)	Heat Gen. (J/g)
NCA	242	878
LCO	256	654
NMC (111)	312	802
NMC (442)	315	744



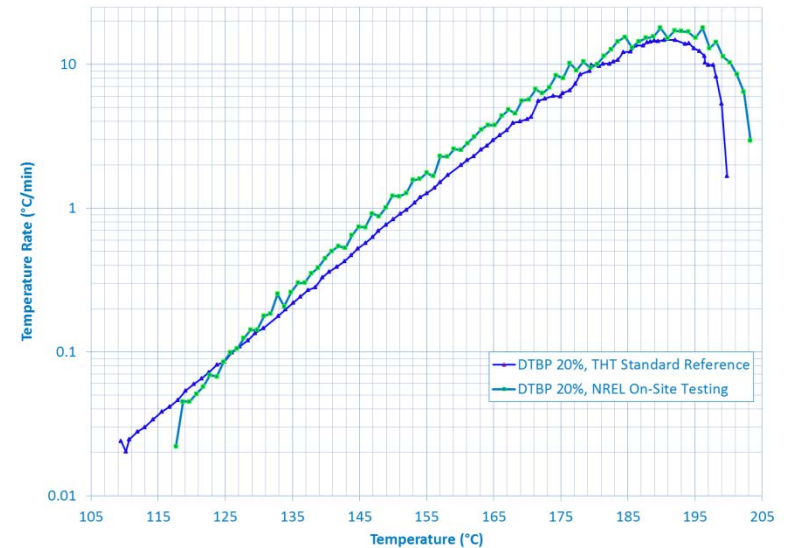
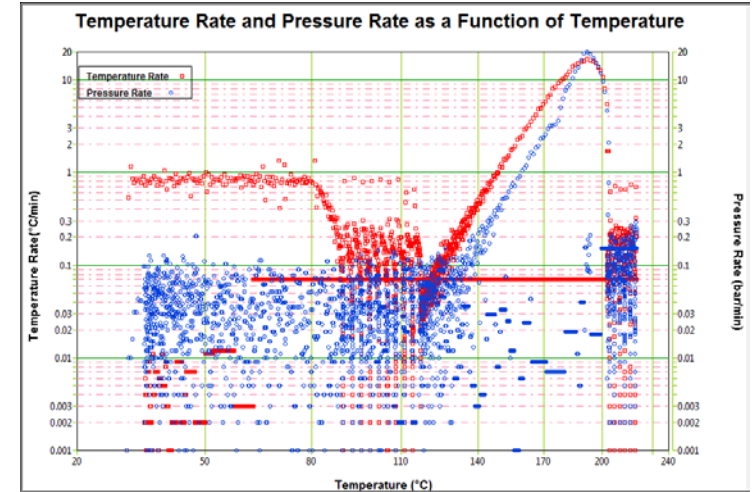
Work in Progress...

Kinetics of Abuse Reactions:

- The evolution of temperature as a function of time is a crucial factor determining the course of response of the cell under abuse.
- Several crucial steps such as the calculation of P_T^1 , the rate expressions for redox reactions involving Ni, Co, and Mn, or the distribution of pressure within the cell, depend on the specific form of the rate expression used to describe the kinetics.
- These factors, in turn, control the temperature evolution.

Approach:

- We are currently exploring two parallel approaches to build the kinetic expressions for the different reactions:
 - Build a lumped model, based on the response of the entire cell (e.g., test a pouch cell inside an ARC chamber and develop time versus pressure/temperature relationships)
 - Measure the characteristic t vs. P (or T) curves for individual reactions under various test conditions and develop model equations that can predict the response of the cell under arbitrary operating conditions.
- Initial setup of these experiments and testing is underway.



Initial setup of the accelerated rate calorimetry (ARC) tests for exploring kinetic mechanism

Related Publications & Presentations

- “Tools for Designing Thermal Management of Batteries in Electric Drive Vehicles,” Ahmad Pesaran, Matt Keyser, Gi-Heon Kim, Shriram Santhanagopalan, Kandler Smith, Advanced Automotive Battery Conference, Pasadena CA, 2013.
- “Safety Modeling of Lithium Ion Batteries,” Shriram Santhanagopalan and Ralph E. White, Invited presentation at the Lithium Battery Technical Experts Meeting at NASA-JSC, Houston TX, 2013.
- “Optimal Control of Li-Ion Batteries Based on Reformulated Models,” Venkat Ramadesigan, Bharat Suthar, Paul Northrop, Shriram Santhanagopalan, Richard Braatz, Venkat Subramanian, 223rd ECS Meeting, Toronto, Canada, 2013.
- “Optimal Control and State Estimation of Lithium-ion Batteries Using Reformulated Models,” Bharat Suthar, Venkat Ramadesigan, Paul Northrop, Shriram Santhanagopalan, Richard Braatz, Venkat Subramanian, American Control Conference, Washington DC, 2013.
- “Impact Response of Lithium Ion Batteries,” S. Santhanagopalan, A. Vlahinos, C. Yang, G.H. Kim, M. Sprague, 224th ECS Meeting , San Francisco CA, 2013.
- “AIAA Battery Standard – Alkaline, NiMH and NiCd Batteries,” Shriram Santhanagopalan and Gi-Heon Kim, Published by the American Institute of Aeronautics and Astronautics, 2013.
- “Thermal Management for Batteries,” Shriram Santhanagopalan, Gi-Heon Kim and Ahmad Pesaran, Invited Chapter in *Lithium Batteries: Recent Trends and Perspectives*, Edited by Gholam Abbas Nazri, Palani Balaya, Ram Manthiram, Atsuo Yamada and Yong Yang, Wiley Publishers, 2014.

Summary & Next Steps

FY13

- We have developed simulation tools to correlate the cell design parameters (e.g., mechanical strength of the pouch seal or cell crimp) with the pressure build-up to capture physical deformation of the cell (e.g., during events like cell venting).
- Versatility of these models was demonstrated using different chemistries and form factors.
- The simulation results capture experimental observations (e.g., location of the origin for mechanical failure for pouch and cylindrical cells).
- Measurement of model parameters is underway.

FY14 and beyond (pending support)

- The cell-level failure models, when integrated into a multi-scale framework, can be used to assess reliability of battery packs, and battery life more accurately.
- The properties of the individual layers (electrode, current collector, separator, etc.) have been used to build corresponding effective properties using a plastic kinematic model with failure; alternate approaches to better represent the physics will be explored.
- Establishing the form of the kinetic rate expressions for different chemistries has been identified as a gap in the existing literature; the modulate DSC and ARC experiments coupled with parameter-extraction routines will enable us to determine the rate constants for the reactions associated with thermal runaway.
- These results will be integrated into existing models (e.g., under the CAEBAT platform) for broader outreach.

Acknowledgements

- **DOE VT Energy Storage Program Support**

- Dave Howell
- Brian Cunningham

- **NREL**

- Chuanbo Yang
- Gi-Heon Kim
- Matt Keyser

- **NASA-JSC**

- Judith Jeevarajan

- **SNL**

- Chris Orendorff

